IOPscience iopscience.iop.org

Home Search Collections Journals About Contact us My IOPscience

Substrate orientation, doping and plasma frequency dependencies of structural defect formation in hydrogen plasma treated silicon

This article has been downloaded from IOPscience. Please scroll down to see the full text article.

2002 J. Phys.: Condens. Matter 14 13037

(http://iopscience.iop.org/0953-8984/14/48/349)

View the table of contents for this issue, or go to the journal homepage for more

Download details:
IP Address: 171.66.16.97
The article was downloaded on 18/05/2010 at 19:15

Please note that terms and conditions apply.

INSTITUTE OF PHYSICS PUBLISHING JOURNAL OF PHYSICS: CONDENSED MATTER

J. Phys.: Condens. Matter **14** (2002) 13037–13045 PII: S0953-8984(02)54095-9

Substrate orientation, doping and plasma frequency dependencies of structural defect formation in hydrogen plasma treated silicon

A G Ulyashin[1], R Job[1], W R Fahrner[1], O Richard[2], H Bender[2], C Claeys[2], E Simoen[2] and D Grambole[3]

[1] Department of Electrical Engineering, University of Hagen, Hagen D-58084, Germany
[2] IMEC, Kapeldreef 75, B-3001 Leuven, Belgium
[3] Forschungszentrum Rossendorf, POB 510119, D-01314 Dresden, Germany

Received 27 September 2002
Published 22 November 2002
Online at stacks.iop.org/JPhysCM/14/13037

Abstract
The formation of structural defects in hydrogen plasma treated (100)- and (111)-oriented p-type Czochralski (Cz) Si and in [100]-oriented n-type Si was studied by Raman spectroscopy, scanning electron microscopy and transmission electron microscopy. The samples were treated either by a 110 MHz or 13.56 MHz hydrogen plasma at 250 °C for 60 min. The distribution of hydrogen was studied by nuclear reaction analysis. It is found that, after the hydrogen plasma treatment, the surface of Cz Si is structured and the roughness of the surface depends on the orientation and doping level of the substrate. The defect density increases for (100)-oriented wafers for the higher plasma frequency but for (111)-oriented wafers it is lower, applying the same hydrogen plasma frequency. Different defect types were found: stacking faults on {111} planes, dislocations and circular shaped defects exhibiting a strong stress field. The formation of nearly free hydrogen molecules (Raman shift of about 4150 cm^{-1}) was observed by Raman spectroscopy after the plasma hydrogenation. It was found that the H_2 molecule concentration depends on the concentration of structural defects. The hydrogen molecules can be formed in both n- and p-type Si, unlike the case of remote plasma hydrogenation.

1. Introduction

The behaviour of hydrogen in silicon has been extensively studied for about 20 years. This was motivated by the capability of hydrogen to passivate defects, deactivate dopants, suppress carrier traps and induce point or extended defects [1, 2]. Recently it was found that hydrogen-terminated structural defects drive the formation of internal surfaces into cracks, where H_2 is evolved, which leads to the blister formation or to exfoliation of the thin Si layers [3–8]. Moreover, in order to explain the mechanism of surface roughening by the hydrogen

plasma treatment a similar model was proposed [9]. According to this model one can state that, when the hydrogen concentration during a plasma treatment exceeds a certain threshold, {111}-oriented platelets are generated since a Si etching reaction occurs preferentially at positions where these platelets intersect the surface. This preferential etching reaction leads to a surface roughening. Based on this phenomenon a technique for the formation of nano-structured Si films using hydrogen plasma treatments of mono-crystalline Si substrates has been developed [10]. With Raman spectroscopy it was also found that the nearly free H_2 molecules appear in nano-voids/platelets after plasma hydrogenation of the silicon samples [11–16]. Both the above-mentioned phenomena are based on the formation and evolution of hydrogen-related cavities or platelets filled with hydrogen atoms either involved in Si–H or H–H bonds. The formation process depends on the concentration of hydrogen and the hydrogenation/annealing temperature. Moreover, it was stated [17, 18] that the formation of hydrogen-induced platelets during plasma treatment is solely controlled by the Fermi-level position and platelets were only observed in hydrogenated n-type Si. In contradiction to this result, it was shown by Raman spectroscopy that the formation of hydrogen molecules in voids/platelets occurs in both n- and p-type hydrogenated Si [16]. From this fact it can be concluded that the nucleation and evolution of these structural defects can be provided by both negatively and positively charged hydrogen atoms, taking into account the amphoteric character of hydrogen in Si [1, 2]. Therefore, one can expect that the microscopic structure of voids/platelets in hydrogenated Si with different types of conductivity might be different. Moreover, the microscopic structure might be different for hydrogenated Si substrates with different orientation. In this paper we want to give a deeper insight into the problems discussed above by a comparison of the experimental Raman results with transmission electron microscopy (TEM) and scanning electron microscopy (SEM) measurements and the nuclear reaction analysis (NRA).

2. Experimental details

Samples for this study were prepared from boron-doped p-type and phosphorus-doped n-type Czochralski (Cz)-grown silicon crystals. For p-type Cz Si, samples with initial resistivities of about 1 Ω cm and orientations (100) and (111) as well as with 12 Ω cm and orientation (100) were used, while for n-type Cz Si, samples with a resistivity of 4.5 Ω cm and (100) orientation were used. Hydrogen plasma treatments of all samples were done in a PECVD set-up for 1 h at a frequency of 110 MHz, a power of 50 W and a hydrogen flux of 200 sccm. For comparison, to check the influence of the plasma frequency on the formation of voids/platelets during hydrogenation, a hydrogen plasma at a frequency of 13.56 MHz, but with other parameters the same, was applied for 1 Ω cm p-type Cz Si material with (100) orientation. During plasma treatments the samples temperature was $\sim$250 °C. Raman measurements were carried out with a Dilor LABRAM Raman system, where a microscope is confocally coupled to a 300 mm focal length spectrograph. The excitation was supplied by an Ar^+ ion laser (487.987 nm, 20 mW). The diameter of the focused laser spot on the sample surface was about 2 μm. The Raman spectra were collected at room temperature by a Peltier cooled CCD detector (collection time: 1200 s, averaging factor: 10). All spectra were normalized to the maximum of the optical Si phonon line at $\sim$520 cm^{-1}, and the background luminescence was subtracted from the data. The subsurface region with structural defects initiated by hydrogenation of the samples was investigated by TEM. The samples were prepared by mechanical thinning followed by ion beam milling with Ar ions. The H concentrations were measured by NRA, using a system described in [19]. SEM measurements were done on a digital field emitter device (LEO DSM 982). The applied operation voltage was 1 kV.

3. Experimental results and discussion

In figures 1(a)–(e) the Raman spectra for Si–H stretching vibration modes obtained for hydrogen treated Cz Si samples are shown. The spectra were normalized to the Si optical phonon line at 520 cm^{-1}. One can see that these lines consist of several sharper components (dotted curves) except for the case shown in figure 1(d). This can be explained by the fact that not only Si–H bonds (Raman shift $\sim$2100 cm^{-1}) can be formed during the hydrogenation but also other hydrogen-related complexes like Si–H_2, Si–H_3 or others [2]. It is necessary to note that the lines at $\sim$2100 cm^{-1} (and also the components of these lines) are relatively shifted in all cases, which reflects the appearance of the different internal stresses in the subsurface region supersaturated by hydrogen. Moreover, the relative intensity values of Si–H vibrations for p-type Si with (111) orientation is lower (figure 1(d)) than in all other cases, which shows the formation of the preferentially {111}-oriented platelets [16, 20] during hydrogenation. Detailed analysis of the polarized Raman scattering spectra of the 2100 cm^{-1} bands for hydrogenated Si was done in [20] and two different types of {111} platelets were found. It can also be concluded that the intensity of the Si–H_x lines in n- and p-type Si with (100)-orientation is comparable (figures 1 (a) and (c)). This result shows that under our process conditions the platelet formation in hydrogenated Si does not depend on the Fermi-level position as was observed in [17, 18] under somewhat different conditions. At the same time, with the increase of the doping level (figures 1(b) and (c)) the Si–H related band becomes narrower and consists most probably only of Si–H and Si–H_2 related vibration modes for the 1 Ω cm material. It can be concluded that the higher boron concentration in Si suppresses the formation of structural defects with dangling bonds terminated by hydrogen.

Figures 2(a)–(e) show Raman spectra for H–H vibration modes obtained for hydrogen-treated Cz Si samples. Again the spectra were normalized to the silicon optical phonon line at 520 cm^{-1}. As can be clearly seen, the Raman lines at about 4150 cm^{-1} (except for the case shown in figure 1(e)) consist of three component (dots) which probably can be attributed to hydrogen molecules in different platelets [20]. Moreover, the formation of para-H_2 molecules with anti-parallel nuclear spins and ortho-H_2 molecules with parallel nuclear spins can also occur [16]. In this case two narrow components can be identified with para- and ortho-H_2 molecules. No essential difference in the intensities of the H_2-related Raman lines for hydrogenated n- or p-type Si occurs. The formation of H_2 molecules is more intensive for (111)-oriented Si. Higher concentration of boron for p-type Si leads to a suppression of the formation of H_2 molecules trapped within the platelets (figures 2(b) and (c)). The rather low intensity of H_2 vibration modes for 13.56 MHz hydrogenated Si shows that a stronger formation of structural defects with hydrogen terminated dangling bonds than the formation of platelets/voids filled by hydrogen molecules occurs as compared to hydrogenation using a 110 MHz plasma generator.

Figure 3 exhibits a typical SEM picture of the surface of a 1h hydrogen plasma treated Cz Si. As can be seen in figure 3 structuring of the Si surface occurs down to the $\sim$100 nm scale and below. Some essential differences in the sizes of surface structures after hydrogenation by plasma occur for different samples used in this work. One can see that the pyramid-like texturing by hydrogen plasma exposure of the (111)-oriented p-type Si occurs, while for the (100)-oriented sample the surface structure look very similar to μc-Si. The sizes of the surface structures depend on the level of doping and on the orientation of the Si substrate. This structuring can be explained by the preferential Si etching by the hydrogen plasma. It leads to a pyramid-shaped surface roughness along {112} planes, as revealed by the cross-section TEM, discussed below. This etching process might be enhanced in the defect regions and depends on the crystallographic structure of the surface. It can be concluded also that the

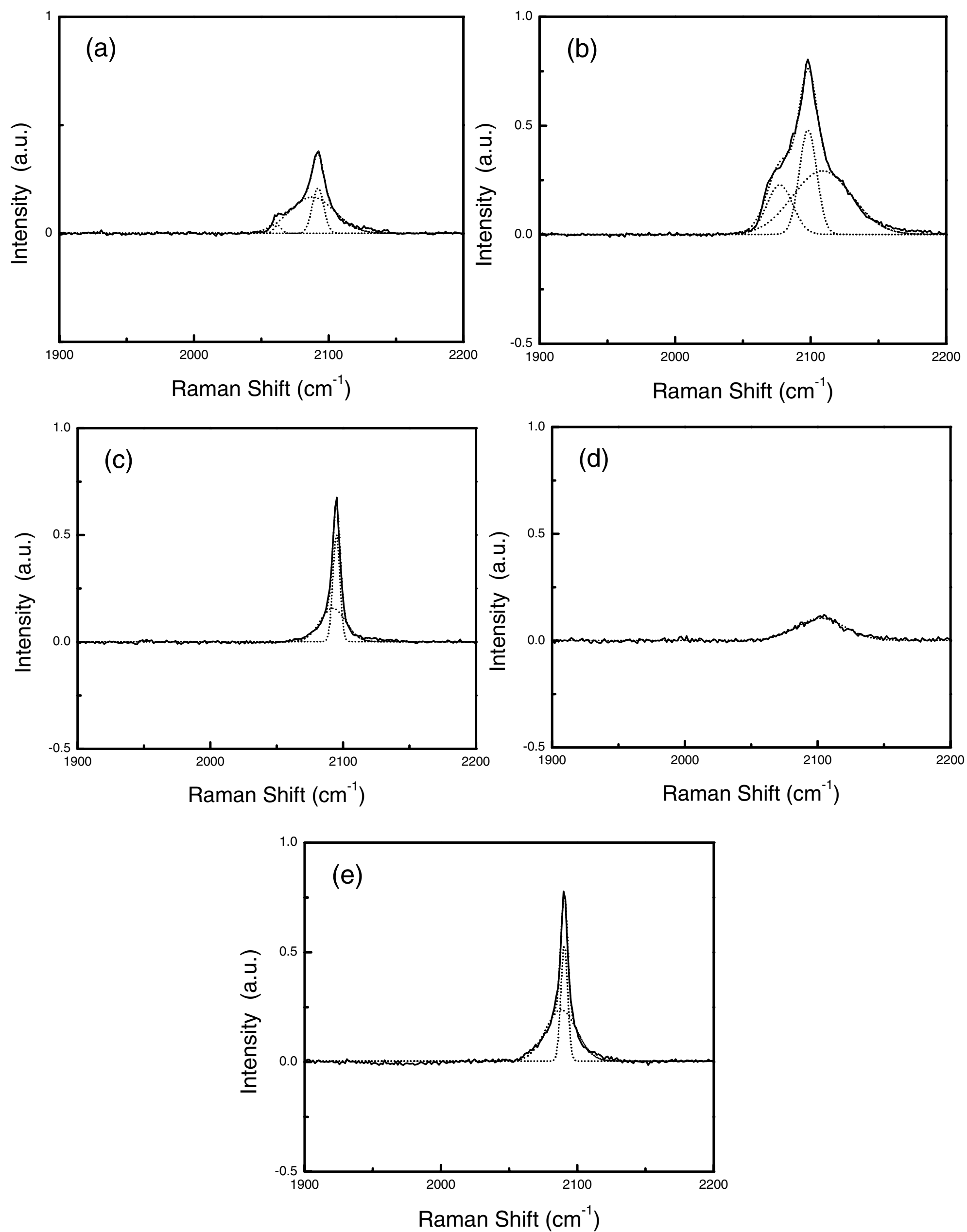

Figure 1. Normalized Raman spectra for stretching vibration Si–H modes: (a)–(d) 110 MHz H plasma treatment, (e) 13.56 MHz H plasma treatment. (a) N-type Cz Si (100) orientation, 4.5 Ω cm; (b) P-type Cz Si (100) orientation, 12 Ω cm; (c) P-type Cz Si (100) orientation, 1 Ω cm; (d) P-type Cz Si (111) orientation, 1 Ω cm; (e) P-type Cz Si (100) orientation, 1 Ω cm

interaction of hydrogen with boron during the structural defect formation processes is one of the key parameters. The density of these defects is very high because of high hydrogen concentration in the subsurface (∼50 nm) layer (figure 4). This high defect density leads to the

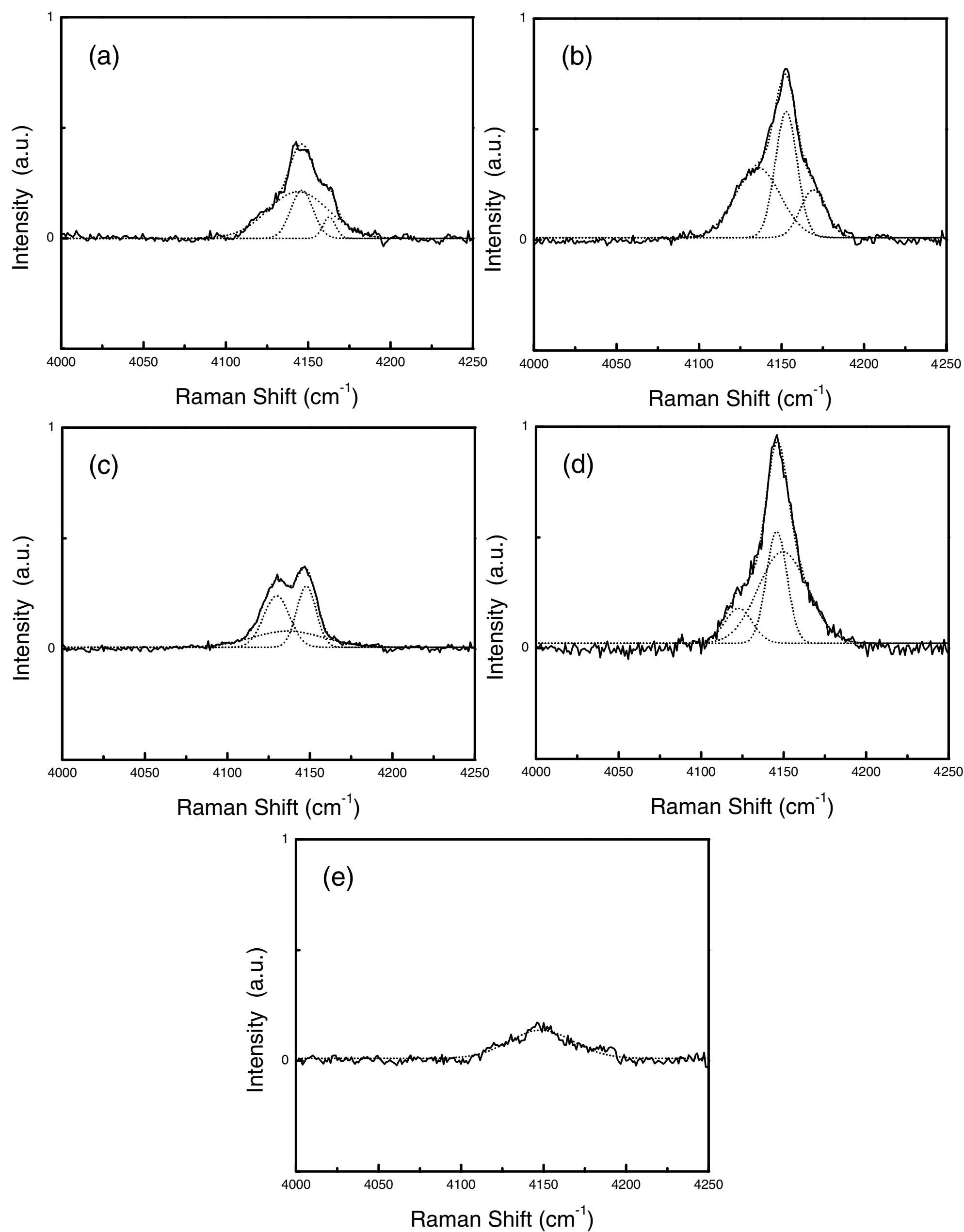

Figure 2. Normalized Raman spectra of H–H bonds: (a)–(d) 110 MHz H plasma treatment, (e) 13.56 MHz H plasma treatment. (a) N-type Cz Si (100) orientation, 4.5 Ω cm; (b) P-type Cz Si (100) orientation, 12 Ω cm; (c) P-type Cz Si (100) orientation, 1 Ω cm; (d) P-type Cz Si (111) orientation, 1 Ω cm; (e) P-type Cz Si (100) orientation, 1 Ω cm.

structuring on the nanoscale. From figure 4 it can also be seen that the hydrogen concentration is nearly the same for different samples up to 200–300 nm depth. Thus, all peculiarities of the platelets/voids formation and surface structuring of hydrogenated Si can be attributed to

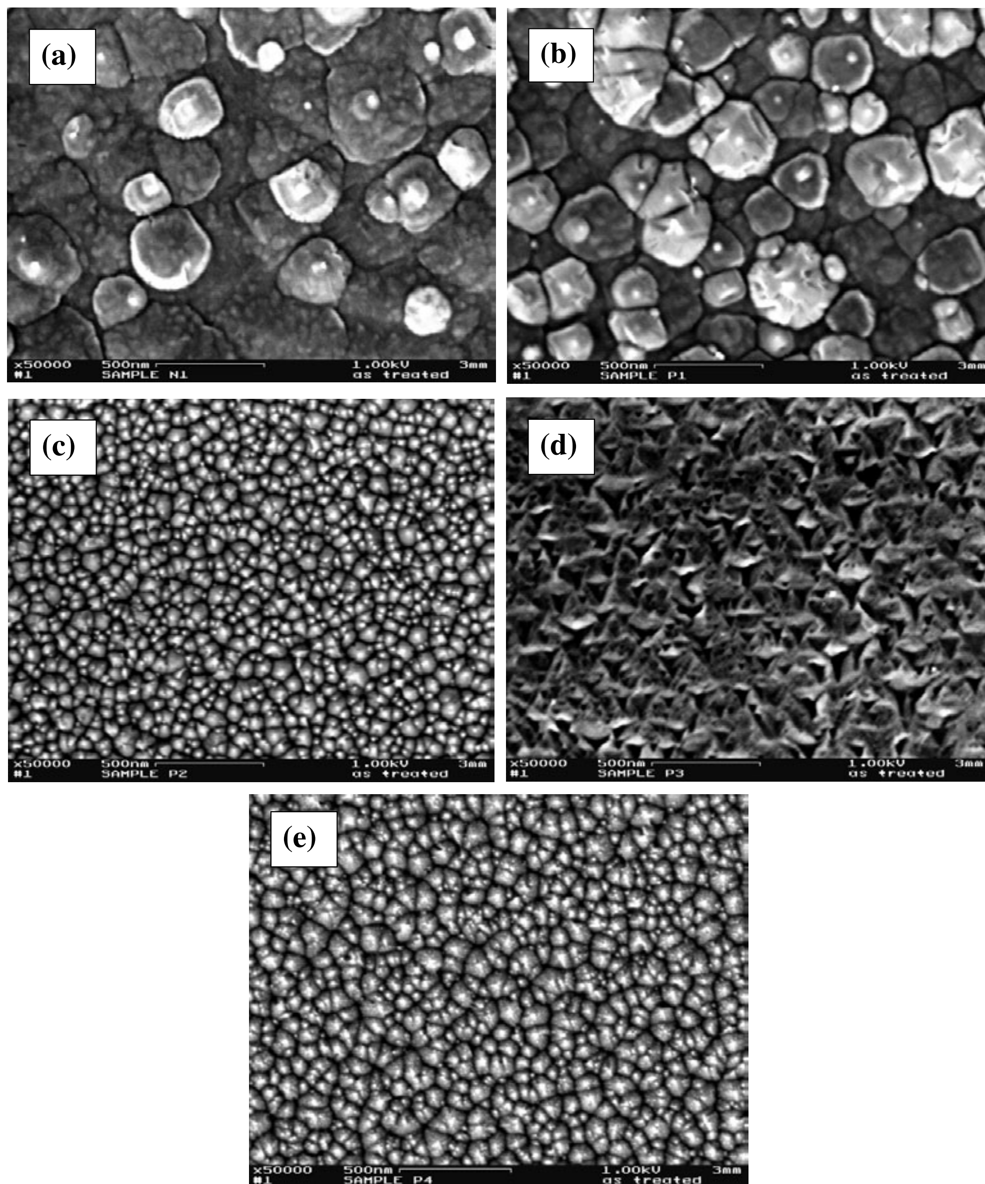

Figure 3. SEM picture of the surface of as-hydrogen plasma treated Cz Si samples: (a)–(d) 110 MHz H plasma treatment, (e) 13.56 MHz H plasma treatment. (a) N-type Cz Si (100) orientation, 4.5 Ω cm; (b) P-type Cz Si (100) orientation, 12 Ω cm; (c) P-type Cz Si (100) orientation, 1 Ω cm; (d) P-type Cz Si (111) orientation, 1 Ω cm; (e) P-type Cz Si (100) orientation, 1 Ω cm.

the differences between substrates (level of doping or orientation). In spite of the amphoteric properties of hydrogen in Si, the formation of these structural defects occurs in both n- and p-type Si.

Figures 5(a)–(e) show typical cross-sectional TEM pictures for the subsurface region of hydrogen plasma treated samples. As can be seen from figure 5 a rather high density of platelets occurs for all cases. Different defect types are present, stacking fault-like defects on

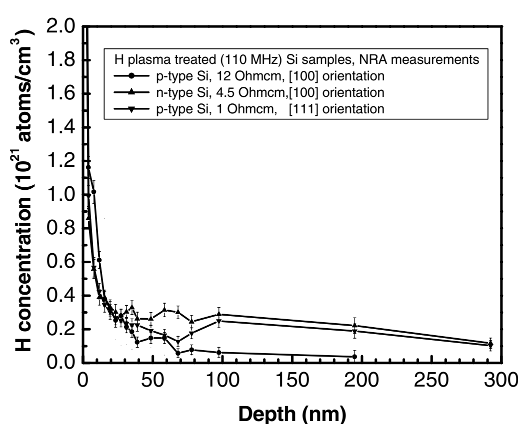

Figure 4. Hydrogen depth distribution in Cz Si samples hydrogenated by a 110 MHz plasma (NRA measurements).

{111} planes, dislocations and circular shaped defects exhibiting a strong stress field. More detailed investigations are necessary to clarify the origin and atomic structure of these defects. The defect density increases with the increase of the plasma frequency and is lower for the (111)-oriented sample applying the same plasma frequency. Moreover, the defect density is lower for higher doped p-type Si, which correlates with the results of Raman measurements.

4. Conclusions

Our experimental results obtained by different methods can be summarized as follows.

Formation of structural defects during hydrogenation does not depend on the Fermi-level position in Cz Si. If the hydrogen concentration in the subsurface region (NRA) is nearly the same, in both n- and p-type Si different structural defects can be formed (Raman, TEM). These structural defects are hydrogen-initiated and are as follows: stacking fault-like defects on {111} planes, dislocations and circular shaped defects exhibiting a strong stress field (TEM). They include different hydrogen-related complexes and also different concentrations of hydrogen molecules (Raman). More detailed investigations are necessary to clarify the origin and atomic structure of these defects. The hydrogen plasma Si etching reaction, preferentially at positions where the platelets intersect the surface, leads to the surface structuring on a nanoscale (SEM).

A high concentration of hydrogen (up to 10^{21} cm^{-3}) occurs within thin (up to $\sim$50 nm depth) subsurface layers of the Si substrates after plasma exposure NRA. Such hydrogen accumulations can also lead to the formation of structural defects fulfilled by hydrogen molecules (Raman) with rather high density and, as a result, to the surface structuring on the nanoscale due to the blistering on a nanoscale SEM. This process can exist in parallel to the preferential etching of areas around platelets. The size of the surface structures depends on the orientation and on the level of doping of the Si substrates (SEM).

The most important parameters, which regulate the structural defect density in deeper (up to 1 μm depth) regions, are the level of the Si substrate doping and the plasma frequency (TEM). Higher boron concentrations suppress the structural defect formation processes as well as a lower hydrogen plasma frequency (TEM).

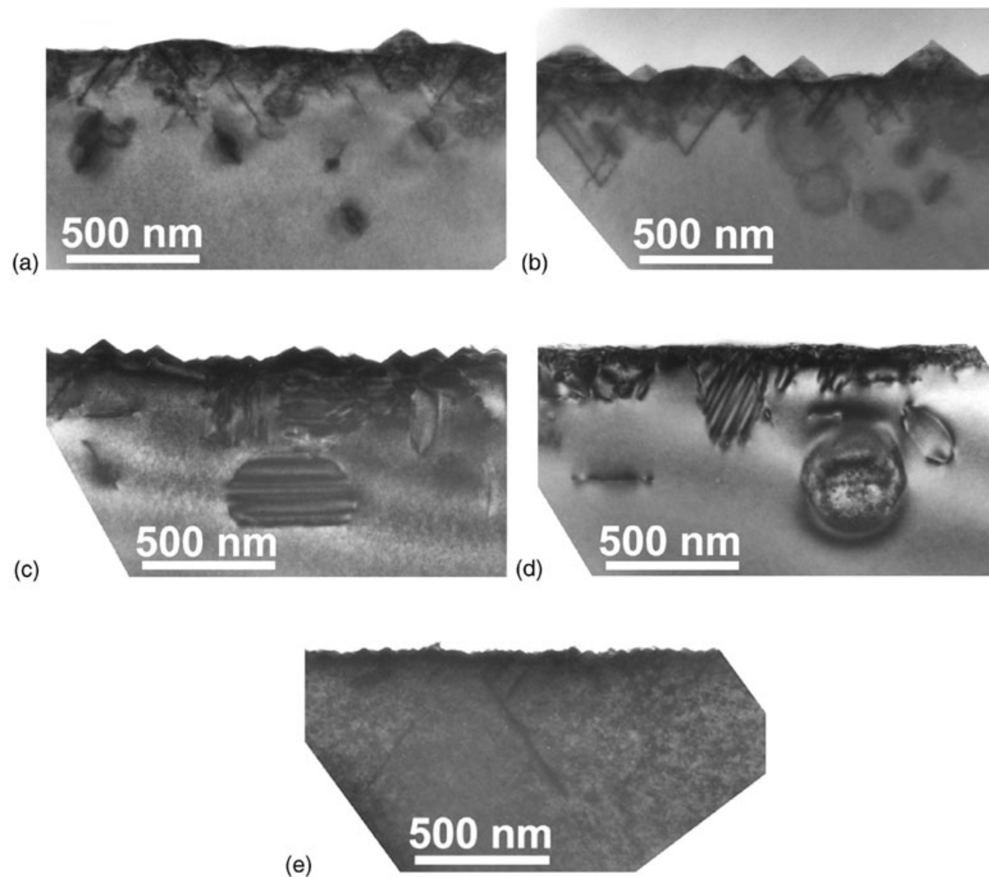

Figure 5. Cross section TEM pictures: (a)–(d) 110 MHz H plasma treatment, (e) 13.56 MHz H plasma treatment. (a) N-type Cz Si (100) orientation, 4.5 Ω cm; (b) P-type Cz Si (100) orientation, 12 Ω cm; (c) P-type Cz Si (100) orientation, 1 Ω cm; (d) P-type Cz Si (111) orientation, 1 Ω cm; (e) P-type Cz Si (100) orientation, 1 Ω cm.

References

[1] Pearton S J, Corbett J M and Stavola M 1992 *Hydrogen in Crystalline Semiconductors* (Berlin: Springer)

[2] Pankove J I and Johnson N M (ed) 1991 *Hydrogen in Semiconductors (Semiconductors and Semimetals 34)* (San Diego, CA: Academic)

[3] Bruel M 1995 *Electron. Lett.* **31** 1201

[4] Grisolia J, Ben Assayag G, Claverie A, Aspar B, Lagahe C and Laanab L 2000 *Appl. Phys. Lett.* **76** 852

[5] Chabal Y I, Weldon M K, Caudano Y, Stefanov B B and Raghavachari K C 1999 *Physica* B **273–274** 152

[6] Lu X, Cheung N W, Strathman M D, Chu P K and Doyle B 1997 *Appl. Phys. Lett.* **71** 1804

[7] Weldon M K, Marsico V E, Chabal Y J, Agarwal A, Eaglesham D J, Sapjeta J, Brown W L, Jacobson D C, Caudano Y, Christman S B and Chaban E E 1997 *J. Vac. Sci. Technol.* B **15** 1065

[8] Weldon M K, Collot M, Chabal Y J, Venezia V C, Agarwal A, Haynes T E, Eaglesham D J, Christman S B and Chaban E E 1998 *Appl. Phys. Lett.* **73** 3721

[9] Hwang K, Yoon E, Whang K and Lee J 1997 *J. Electrochem. Soc.* **144** 335

[10] Fahrner W R, Job R and Ulyashin A G 2001 *Proc. 2001 1st IEEE Conf. Nanotechn.* (Piscataway, NJ: IEEE) p 282

[11] Murakami K, Fukata N, Sasaki S, Ishioka K, Kitajima M, Fujimura S, Kikuchi J and Haneda H 1996 *Phys. Rev. Lett.* **77** 316

[12] Nakamura K G, Ishioka K, Kitajima M and Murakami K 1997 *Solid State Commun.* **101** 735

[13] Leitch A W R, Alex V and Weber J 1998 *Phys. Rev. Lett.* **81** 421

[14] Job R, Ulyashin A G and Fahrner W R 2001 *Mater. Sci. Semicond. Proc.* **4** 257

[15] Ulyashin A G, Job R, Fahrner W R, Grambole D and Herrmann F 2002 *Solid State Phenom.* **82–84** 315

[16] Job R, Ulyashin A G and Fahrner W R 2002 *Solid State Phenom.* **82–84** 139

[17] Nickel N H, Anderson G B, Johnson N M and Walker J 1999 *Physica* B **273–274** 212

[18] Nickel N H, Anderson G B, Johnson N M and Walker J 2000 *Phys. Rev.* B **62** 8012

[19] Rudolph W, Grambole D, Groetzschel R, Heiser C, Herrmann F, Knothe P and Neelmeijer C 1988 *Nucl. Instrum. Methods* B **33** 803

[20] Lavrov E V and Weber J 2001 *Physica* B **308–310** 151